International Journal of Control, Automation and Systems 20(1) (2022) 232-242
http://dx.doi.org/10.1007/s12555-020-0980-x
ISSN:1598-6446 eISSN:2005-4092
http://www.springer.com/12555

Optimization and Comparison of Typical Elastic Actuators in Powered Ankle-foot Prosthesis

Jingjing Liu, Noor Azuan Abu Osman*, Mouaz Al Kouzbary, Hamza Al Kouzbary, Nasrul Anuar Abd Razak, Hanie Nadia Shasmin, and Nooranida Arifin

Abstract: Elastic actuators are broadly applied in the design of the powered ankle-foot prosthesis, so it is a significant task to select and optimize a suitable elastic actuator. Dynamic models of seven kinds of elastic actuators are constructed from a two-degrees-of-freedom vibration system in rotation. With input parameters from sound ankle data during walking, motor data, and the three-dimensional model of the proposed prosthesis, two objectives, which are to minimize the peak mechanical power and mean energy consumption power of the motor, respectively, are optimized by changing the parameters of elastic elements. Unidirectional parallel elastic actuator (UPEA) and UPEA with series spring (SE+UPEA) optimize nearly 75% compared to the direct-driver actuator (DDA) in minimizing the characteristic of peak mechanical power. When it comes to reducing mean energy consumption power, UPEA is also the best, and its performance is at least 15% better than those of the other four kinds of elastic actuators with effective optimization. Besides, features of torque and velocity on the driver end are also compared from elastic actuators to sound ankle. The comparison contributes to understanding the optimization mechanism of different elastic elements, and the optimized and compared performances of elastic actuators can be utilized as the selection basis in the design of the powered ankle-foot prosthesis.

Keywords: Dynamics, elastic actuators, optimization, powered ankle-foot prosthesis.

1. INTRODUCTION

With the series elastic actuator (SEA) being first designed in 1995 [1], the emergence of various elastic actuators has changed people's minds on the view that the more rigid the transmission mechanism, the better its performance. The application of elastic actuators has expanded from the threshold of humanoid robotics to fields related to rehabilitation equipment, such as a robot for back-pain rehabilitation [2], and various prostheses, which are relevant to the human body. These high-performance actuators gained considerable attention after the concept of the powered ankle-foot prosthesis was proposed. Statistical data from the previous review show that, among 94 powered ankle-foot prostheses developed since 2000, those with elastic actuators account for more than 40% [3]. There is a successfully commercialized prosthesis, named Walk-Run Ankle (SpringActive), employing a SEA [4]. To develop a powered ankle-foot prosthesis, developers and researchers always encounter an inevitable problem, that is, how to select a suitable elastic actuator and determine its parameters. Hence, among various elastic actuators, it is of great significance to compare their noteworthy performances in the operation of the prosthesis and improve them by optimizing the corresponding parameters of elastic elements.

Although the number of previous studies related to powered ankle-foot prostheses driven by elastic actuators is large, only a few have optimized the stiffness of spring in the design. In [5], the stiffness of series spring is selected according to the analysis of shock loads at heel strike, and a parallel spring with optimized stiffness is applied to meet the requirements of force bandwidth. During the design of the ankle joint of a transfemoral prosthesis, Fu *et al*. [6] optimized the stiffness of series spring in a reasonable range, in which the bandwidth of the mechanical open-loop system is large enough, to minimize the energy cost of transport. Hitt [7] optimized the stiffness of the series spring to minimize the peak motor power. Reference [8] provides a prosthesis with restructuration for dancers, and the stiffness, equilibrium angle, and damping of a U-shape series spring are selected following the feedback from the amputee participants regarding performance and comfort while executing dance steps. Sha *et al*.

Manuscript received December 29, 2020; revised February 15, 2021; accepted March 12, 2021. Recommended by Associate Editor Yangmin Li under the direction of Editor Won-jong Kim. This work was funded by PlaTCOM HIP-2 (AIM/PlaTCOM/HIP2/CCGF/2017/168).

Jingjing Liu, Noor Azuan Abu Osman, Mouaz Al Kouzbary, Hamza Al Kouzbary, Nasrul Anuar Abd Razak, Hanie Nadia Shasmin, and Nooranida Arifin are with the Centre for Applied Biomechanics, Department of Biomedical Engineering, Faculty of Engineering, University of Malaya, Kuala Lumpur 50603, Malaysia (e-mails: kva190023@siswa.um.edu.my, azuan@um.edu.my, {kva190025, kga170032}@siswa.um.edu.my, {nasrul.anuar, hanie_nadia, anidaum}@um.edu.my).
* Corresponding author.

[9] tried to minimize ankle torque by optimizing the stiffness of the torsional spring in their ankle-foot prosthesis via a virtual prototype in ADAMS.

Similarly, the literature related to the comparison among different kinds of elastic actuators is also insufficient. On the aspect of general elastic actuators, [10] compares three kinds of dynamic behaviors, that is, force sensitivity, compliance, and transmissibility in three different locations of series spring in SEA, and the results showed that the location of series spring has a significant influence on the performance of abovementioned assessment criteria. Verstraten *et al*. [11] investigated the energy efficiency of SEA and parallel elastic actuator (PEA), including mechanical peak power, and mechanical and electrical energy consumption, in a case of a sinusoidal motion to a pendulum load. Their results contribute to a very clear relationship between the three targets and pendulum swinging frequency and spring stiffness and provide significant evidence to make a choice between SEA and PEA.

On the other aspect of elastic actuators in the field of the ankle-foot prosthesis especially, two papers from the research group of Martin Grimmer [12,13] compare several actuators under different walking and running speeds. Reference [12] compared the direct-driver actuator (DDA), SEA, PEA, PEA with a series elastic element (SE+PEA) and double SEA; the other focused on the mechanism of SEA, SEA with a parallel elastic element (PE+SEA), SEA with the unidirectional parallel elastic element (UPE+SEA), PEA, and unidirectional parallel elastic actuator (UPEA). Both papers employed the exhaustivity method in the selection of spring stiffness to identify optimized performances in these elastic actuators. However, it is worth noting that the dynamic models in [12,13] only involve the elements of force and displacement. In some of newer references, the dynamic model has been expanded to include inertia of motor and load to analyze SEA in [14,15], and the significance of the expansion has been approved via a uniformization model of SEA in [16]. However, similar expansion has not been reported in other kinds of elastic actuators.

From the above review, it is not difficult to find that it is still a challenge about the selection and parameters optimization to apply an elastic actuator in the design of the powered ankle-foot prosthesis. Reasons to the challenge mainly come from the following points: a) the types of elastic actuators compared and optimized in previous studies are incomplete; b) the incomplete dynamic models of elastic actuators may make an influence on the accuracy of the analysis results; c) the comparison and optimization of elastic actuators in different prosthesis structures cause the low comparability from one study to others; d) the different optimization objectives and working conditions also reduce the reference value in the future design.

Therefore, to provide more complete and accurate evidence to select a suitable elastic actuator and optimize its parameters in the future design of the powered ankle-foot prosthesis, this study will expand on the dynamic models of each kind of elastic actuator to include inertia. To avoid the impact of different transmission mechanisms and arrangement, the comparison and optimization of all seven typical elastic actuators will be based on the same basic structure, where a torsional spring will be employed to simplify the arrangement, instead of compressional/extensional elastic elements.

This paper is arranged as follows: The first emphasis is to construct expanded dynamic models of elastic actuators and DDA in the application of power ankle-foot prosthesis. Parameters of elastic elements in elastic actuators are optimized to achieve the optimizing objectives after the determination of input parameters. Finally, optimal performances of actuators are analyzed and compared to understand how the optimization is completed by different elastic elements.

2. METHODS

2.1. Dynamic models

A two-degrees-of-freedom (DoF) vibration system in rotation consists of two main bodies with rotational inertia, three torsional springs, and three dampers, is illustrated in Fig. 1(a). Based on the simplification of the 2-DoF system, this paper introduces dynamic models for seven kinds of elastic actuators and DDA, namely, a rigid actuator without any elastic element. With these models, dynamics equations can be deduced easily according to Newton-Euler Equations and Hooke's Law.

2.1.1 Series elastic actuator

The SEA can be abstracted as the model that includes only one torsional spring between a driver end (the first rotational-inertia body) and a load end (the second one), same as below, shown in Fig. 1(b). The driver end contains a motor and transmission. The damping property of the motor works as a damper connected to the rack of the system. The dynamics equations are as follows:

$$J_1\ddot{\theta}_1 = \tau_1 + T_B + T_s, \tag{1}$$

$$J_2\ddot{\theta}_2 = \tau_2 - T_s, \tag{2}$$

where J_1 and J_2 are the rotational inertias or the equivalent ones of the driver and the load ends, respectively, τ_1 is the torque on the driver end, i.e., the torque outputted by the transmission mechanism, τ_2 is the torque on the load end, θ_1 and θ_2 are the angular displacements of both ends, correspondingly, $\dot{\theta}_i$ and $\ddot{\theta}_i$ ($i = 1$ or 2) are the angular velocity and acceleration, and T_B and T_S that are the torques produced by damper and series torsional spring can be calculated based on Hooke's Law.

$$T_B = -B_1\dot{\theta}_1, \tag{3}$$

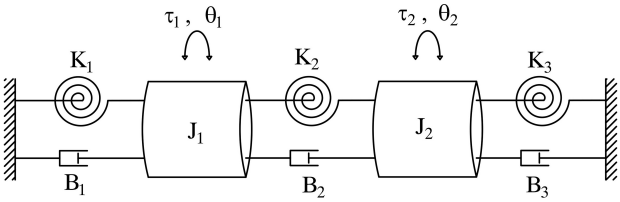

(a) 2-DoF vibration system in rotation.

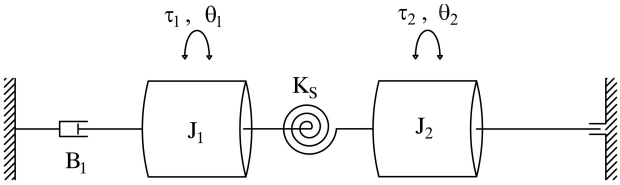

(b) SEA or DDA ($K_S \to \infty$).

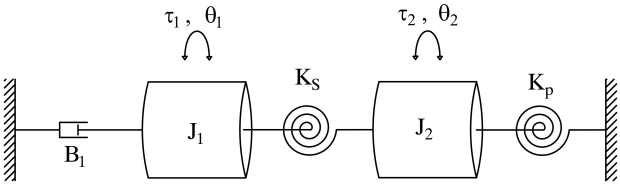

(c) PE+SEA or UPE+SEA (when a unidirectional parallel spring is employed).

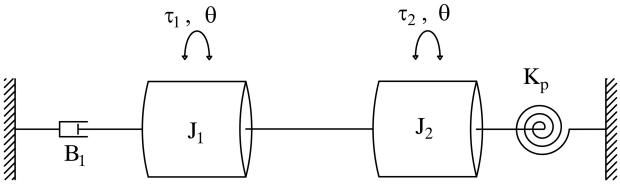

(d) PEA or UPEA (when a unidirectional parallel spring is employed) or DDA ($K_P = 0$).

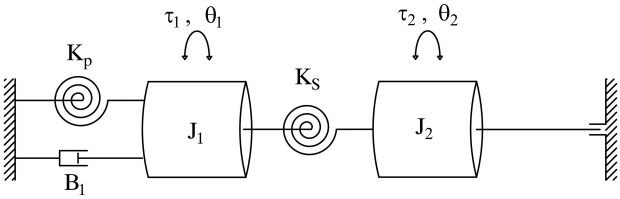

(e) SE+PEA or SE+UPEA (when a unidirectional parallel spring is employed).

Fig. 1. Dynamic models of 2-DoF system, elastic actuators, and a rigid actuator.

$$T_S = -K_S(\theta_1 - \theta_2), \tag{4}$$

where B_1 is the damping coefficient of the motor and K_S is the stiffness of the series spring.

In designing an ankle-foot prosthesis, the torque on the ankle and the ankle angular displacement (or ankle position), i.e., τ_2 and θ_2 on the load end are required to follow the data of the sound ankle and walking parameters as similarly as possible. The angular displacement of the driver end can be solved by (2).

$$\theta_{1,SEA} = (-\tau_2 + J_2\ddot{\theta}_2 + K_S\theta_2)/K_S. \tag{5}$$

$\dot{\theta}_1$ and $\ddot{\theta}_1$ are calculated by taking the first and second derivatives of both sides of (5), and then all results are inputted into (1) to solve the torque on the driver end:

$$\tau_{1,SEA} = J_1\ddot{\theta}_1 + B_1\dot{\theta}_1 + K_S(\theta_1 - \theta_2). \tag{6}$$

2.1.2 Series elastic actuator with parallel elastic element

The PE+SEA adds a parallel torsional spring between the load end and the rack on the SEA, as shown in Fig. 1(c). In this assembly, the parallel spring is not allowed to be preloaded. Namely, the equilibrium position of the parallel spring must be at zero of the ankle joint. Otherwise, the preload will act on the load end to drive it to rotate. The dynamics equation of the driver end is the same as (1), and the torque of parallel spring, T_P, is included in the dynamics equation of the load end:

$$J_2\ddot{\theta}_2 = \tau_2 - T_S + T_P, \tag{7}$$

$$T_P = -K_P\theta_2, \tag{8}$$

where K_P is the stiffness of the parallel spring. The same process of calculation from the SEA model can be engaged to obtain $\theta_{1,PE+SEA}$ and $\tau_{1,PE+SEA}$.

2.1.3 Series elastic actuator with unidirectional parallel elastic element

When the parallel spring in PE+SEA possesses a free end and a fixed one, instead of two fixed ones, it becomes an application of a unidirectional parallel elastic element (UPE or UPS). In this case, the load end of UPE+SEA can only compress the UPE rather than extend it. In comparison with PE+SEA, when T_{UP} that refers to the torque produced by UPE replaces T_P, the dynamics equation of the load end is shown in (9).

$$J_2\ddot{\theta}_2 = \tau_2 - T_S + T_{UP}. \tag{9}$$

In this study, only the positive compression direction (dorsiflexion) of UPE is considered because the ankle torque maximum happens in the dorsiflexion of gait. T_{UP} is expressed by a piecewise function.

$$T_{UP} = \begin{cases} 0, & (\theta_2 \le \theta_{UP}), \\ -K_P(\theta_2 - \theta_{UP}), & (\theta_2 > \theta_{UP}), \end{cases} \tag{10}$$

where θ_{UP} is the equilibrium position of UPE. In UPE+SEA, θ_{UP} must not be negative so that there will be no preload acting on the UPE. Based on the equation set (5), (9), and (10), the angular displacement of and the torque on the driver end, $\theta_{1,UPE+SEA}$ and $\tau_{1,UPE+SEA}$, can be solved.

2.1.4 Parallel elastic actuator

It is not easy to deduce the dynamics equation of the PEA model directly, so this study utilizes a limitation method to obtain the PEA model. From Fig. 1(c) to Fig. 1(d), when the stiffness of the series spring is limited to the positive infinity, the transmission from the driver end to the load end can be regarded as a rigid one, that is, the driver and load end are considered to become one rigid body. Hence, $\theta_1 = \theta_2 = \theta$ in the PEA. In this case, it is equivalent when the parallel spring is connected from the rack to the load end or the driver end. For ease of understanding, the location is selected, as shown in Fig. 1(d) in this paper. The dynamics equation of the PEA model can be deduced from that of PE+SEA when the terms T_S in (1) and (7) are eliminated. It is worth noting that the term T_P in the dynamics equation of PEA is different from that of PE+SEA in (8).

$$(J_1 + J_2)\ddot{\theta} = \tau_1 + \tau_2 + T_B + T_P, \tag{11}$$

$$T_P = -K_P(\theta - \theta_P), \tag{12}$$

where θ_P is the initial equilibrium position of the parallel spring. The preload of the parallel spring that is determined by θ_P can exist in this actuator because the motor can be controlled to hold its initial position. $\tau_{1,PEA}$ can be solved from (11) and (12).

2.1.5 Unidirectional parallel elastic actuator

The model of UPEA is evolved from PEA when a UPE is applied to replace the parallel spring or from UPE+SEA when the stiffness of the series spring tends to be positive infinity. The dynamics equation is shown in (13).

$$(J_1 + J_2)\ddot{\theta} = \tau_1 + \tau_2 + T_B + T_{UP}. \tag{13}$$

Here, T_{UP} is the same as (10). However, the parameter of θ_{UP} can be set in the full range of ankle position. When $\theta_{UP} < 0$, the setup provides a preload of UPE.

2.1.6 Parallel elastic actuator with series elastic element

SE+PEA is an actuator that has an additional series spring connecting between the output end of PEA to the load end. The difference between the SE+PEA and the PE+SEA is the location of the parallel spring, which is between the rack and the driver end in SE+PEA. Therefore, SE+PEA can also be regarded as the other extension based on SEA, where a parallel spring is applied in the location. The abstraction of SE+PEA is shown in Fig. 1(e). With considering the initial equilibrium position of the parallel spring, θ_P, the dynamics equations are deduced as follows.

$$J_1\ddot{\theta}_1 = \tau_1 + T_B + T_S + T_P, \tag{14}$$

$$J_2\ddot{\theta}_2 = \tau_2 - T_S, \tag{15}$$

where T_B and T_S are the same as above, and T_P is similar to (12).

$$T_P = -K_P(\theta_1 - \theta_P). \tag{16}$$

2.1.7 Unidirectional parallel elastic actuator with series elastic element

SE+UPEA employs a series spring at the output end of UPEA, and it can also be understood from SE+PEA when the parallel spring is replaced with a UPE. Therefore, the item T_P is replaced with T_{UP} in (14) to obtain the dynamics equation of the driver end, while the dynamics equation of the load end, (15), does not change.

$$J_1\ddot{\theta}_1 = \tau_1 + T_B + T_S + T_{UP}, \tag{17}$$

where T_{UP} is decided by the angular position of the driver end, the stiffness of UPE, and its equilibrium position θ_{UP} which is also full-ranged as that in UPEA.

$$T_{UP} = \begin{cases} 0, & (\theta_1 \le \theta_{UP}), \\ -K_P(\theta_1 - \theta_{UP}), & (\theta_1 > \theta_{UP}). \end{cases} \tag{18}$$

2.1.8 Direct-driver actuator

The dynamics equation of DDA can be set up in two ways. On the one hand, the equation can be based on a SEA model. The treatment process to evolve from SEA to DDA is the same as that from PE+SEA to PEA. With the stiffness of series spring (K_S) limits to positive infinity, the result from (1) and (2) after eliminating the term T_S is the dynamics equation of DDA. On the other hand, the model of DDA can be based on a PEA model that assigns the stiffness of the parallel spring (K_P) to zero in (12). The dynamics equation can be obtained as (19).

$$(J_1 + J_2)\ddot{\theta} = \tau_1 + \tau_2 + T_B. \tag{19}$$

2.2. Optimization objectives and method

Generally, the peak mechanical power of the motor required in the application, which decides the size and weight of the motor, is the basis to select the motor. In addition, the mean power of energy consumption is also an important index in the application of powered ankle-foot prosthesis. Hence, the research target of this paper is to minimize the peak mechanical power (P_{M,i_MAX}) or the mean energy consumption power ($\bar{P}_{M,i}$) of the motor in each kind of elastic actuator (i = SEA, PE+SEA, UPE+SEA, PEA, UPEA, SE+PEA, SE+UPEA, or DDA) by optimizing relevant parameters of elastic elements, that is, K_S, K_P, θ_P, or θ_{UP} in the abovementioned dynamic models. Both optimization objectives are calculated based on the mechanical power of the driver end during the gait cycle.

$$P_{1,i} = \tau_{1,i}\dot{\theta}_{i,1}. \tag{20}$$

During the operation of the ankle-foot prosthesis, the positive value (negative value) of the motor power means the motor torque is in the same (opposite) direction of the angular velocity because the motor cannot provide negative power. Hence, the objectives to be optimized are constructed by eliminating the influence of direction.

$$P_{M,i\_MAX} = max(|P_{M,i}|) = max(|P_{1,i}/\eta_T|), \tag{21}$$

$$\bar{P}_{M,i} = \left[\int_0^{t_0} (\tau_M^2 R/K_t^2 + |P_{M,i}|)dt\right]/t_0, \tag{22}$$

$$\tau_M = \tau_1/i_0, \tag{23}$$

where η_T is the total efficiency of the transmission, $max(x)$ is utilized to find the maximum of variable x, $|x|$ is the absolute value of variable x, τ_M is the torque produced by the motor, i_0 is the total reduction ratio, R is the motor terminal resistance, K_t is the motor torque constant, and t_0 is the time length of a single gait cycle. (22) is based on [14].

During the process of optimization in this work, it is assumed that the work status of the motor will remain a continuous operation, instead of an intermittent operation, to achieve the desired ankle track during the gait, which is based on some advanced control systems, such as a genetic rule-based fuzzy control system (GRFCS) that is described and verified in [17]. With optimized parameters, the angular velocity, torque, and power of elastic and rigid actuators will be simulated and compared with the counterparts of the sound ankle. In addition, the optimization objectives and other three performances of elastic actuators–peak motor torque (τ_{M,i_MAX}), peak motor speed ($\dot{\theta}_{M,i\_MAX}$), and standard deviation of motor speed ($\sigma(\dot{\theta}_{M,i})$) will be compared with those of DDA.

The dynamics equations of the different actuators and the equations of optimization and comparison processes are constructed as high-order open-loop simulation models in Simulink (The MathWorks, Inc.), where the models of PEA, UPEA, and DDA are second-order, and others are fourth-order. No derivative block is employed in the construction because the block in Simulink is completed by the finite difference method, which has great errors among different sizes of the simulation step. Curve Fitting Toolbox (MATLAB) is applied to fit input time-varying parameters with an integrated or segmented function, and then each order derivation of the parameters can be calculated mathematically. Response Optimizer Toolbox (Simulink) is utilized to complete the optimization.

2.3. Parameters

First, data from sound ankle during walking are utilized as the input parameters on the load end. The angular displacement (θ_2) and ankle torque (τ_{Ankle}) stem from [18] are shown in Fig. 2, where the dorsiflexion and plantarflexion are in positive and negative directions, respectively. The data were collected under the self-selected

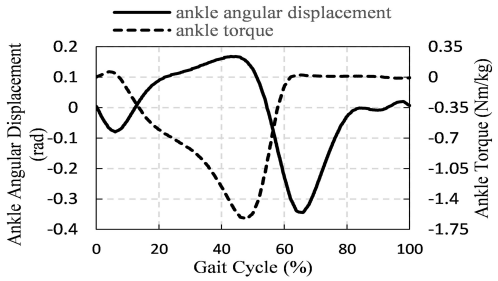

Fig. 2. Ankle angular displacement and torque of normal walking, and data stem from [18].

walking speed, the average of which is about 1.5 m/s, and the mean weight of subjects is 75 kg.

The dynamic stiffness, dynamic damping, and inertia of the ankle in three different stages of walking are provided by [19–21], respectively. During the stance phase of walking, perturbations were applied by a mechatronic platform, termed the Perturberator Robot in [19,21], and then the three impedance parameters of the ankle during the stance phase were estimated using least squares estimation based on (24):

$$T_P = I_{tot}\ddot{\theta}_{AP} + b_a\dot{\theta}_{AP} + k_a\theta_{AP}, \tag{24}$$

where T_P is the torque response to the perturbation, I_{tot} is the total inertia of the foot and other coupled body segments, b_a and k_a are the damping and stiffness coefficients of impedance, respectively, θ_{AP}, $\dot{\theta}_{AP}$, and $\ddot{\theta}_{AP}$ are the angular perturbation displacement of the ankle and its first and second derivatives.

A wearable ankle robot, Anklebot, was applied to complement the aforementioned research during the swing and early stance phase of walking in [20]. The specific research and experimental methods from the same literature will not be reiterated in detail here. It is worth noting that the result of inertia provided in [20] was the summation of the inertia at the ankle and that of the Anklebot. Therefore, to obtain the inertia at the ankle solely during the studied period, this study estimates the inertia of the Anklebot according to the information from [22]. In this paper, the rotational inertia of sound ankle is regarded as the counterpart of the load end, J_2, because of the high similarity of an ankle-foot prosthesis, the size and weight of which are usually well-designed to the replaced sound segment. The results of dynamic stiffness (K_{Ankle}), dynamic damping (B_{Ankle}), and inertia (J_2) are merged and shown in Fig. 3.

With all the abovementioned data of sound ankle, the torque on the load end, τ_2, is calculated by (25), and the result is shown in Fig. 4. In addition, a gait cycle of an adult is in the range of 1.0 s to 1.3 s, and the value of t_0 referred to [23] is selected as 1.13 s.

$$\tau_2 = J_2\ddot{\theta}_2 + B_{Ankle}\dot{\theta}_2 + K_{Ankle}\theta_2 - \tau_{Ankle}. \tag{25}$$

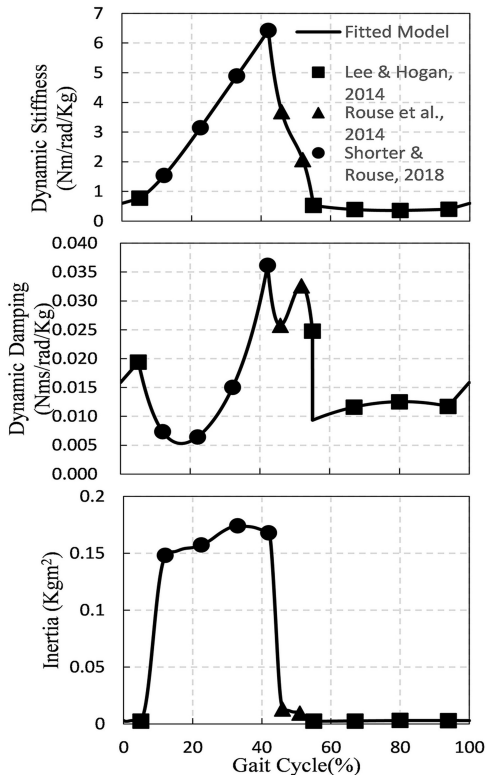

Fig. 3. Dynamic stiffness, damping, and inertia of ankle during normal walking, and data stem from [19–21].

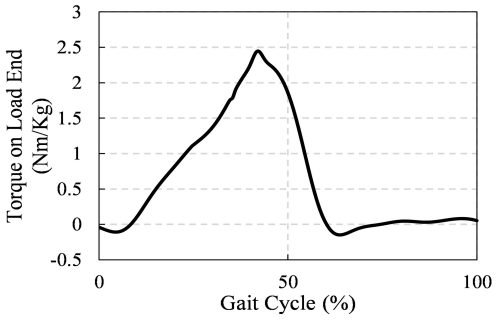

Fig. 4. Calculation result of torque on the load end.

Second, parameters of motor and transmission are selected. A 200 w motor, Maxon EC-4pole 30 brushless 305013 motor, which has a mass of 300 g and a size of ϕ30 mm×98.5 mm, is selected according to the most rated power for a brushless motor mentioned in previous literature [5,6,24,25]. The calculated damping coefficient of the motor is 5.66×10^{-6} Nm·s/rad, and the intermittent output torque can reach 0.25 Nm at least. The motor terminal resistance (R) and the motor torque constant (K_t) can be learned from the official datasheet. When a user weights 75 kg and the security coefficient is 1.5, the total reduction ratio of the transmission needs to reach 733.5:1 and above.

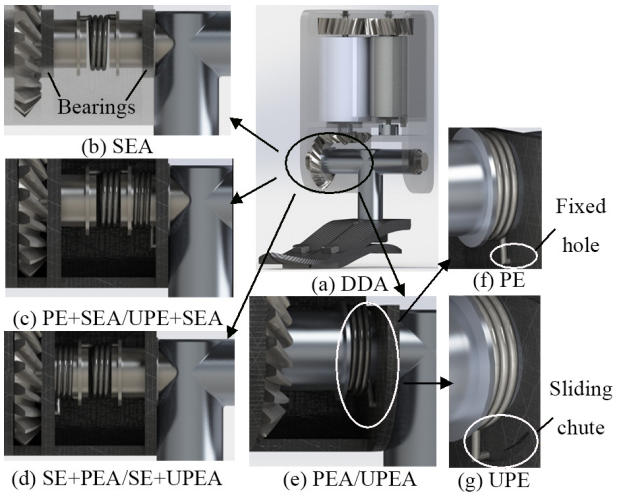

Fig. 5. Conceptual models of powered ankle-foot prosthesis with different actuators.

Therefore, a four-stage planetary gearbox (Once Top Motor), which possesses a reduction ratio of 594.6:1, a mass of 490 g, and a size of ϕ42 mm×93 mm, works together with a pair of gears in parallel axes and a pair of bevel gears in orthogonal axes. Finally, the total reduction ratio i_0 reaches the value of 742.7:1.

Conceptual models of the prosthesis with different elastic elements are shown in Fig. 5. In the model of DDA, Fig. 5(a), the shank shell that is worked as the rack in the prosthesis is transparent to show interior components clearly. Similarly, the modified shell is also transparent in the model of SEA, Fig. 5(b), to show two additional bearings. The two bearings are designed in any elastic actuators involving series spring (SEA, PE+SEA, UPE+SEA, SE+PEA, and SE+UPEA) because in the conceptual structures of these actuators, the output shaft of the transmission and the shaft of the ankle are divided into different parts, and the series spring is utilized to connect each other. On the aspect of the normal or unidirectional parallel elastic element, one end of the torsion spring is fixed to the corresponding shaft. The other end is connected to the shell, namely the rack, by two different methods depending on the type of parallel spring, shown in Fig. 5(f) and 5(g), respectively. For a parallel elastic element (PE), the end is also fixed on the rack; for a unidirectional parallel elastic element (UPE), the end slides in a chute during the operation of the prosthesis.

Based on these 3D models, the rotational inertia on the load end (J_1) that is converted the inertia of transmission components to the final output shaft is 9.61×10^{-5} kg·m^2. The J_1 will be utilized in every elastic actuator because the influence of elastic elements can be ignored by their lightweights. After meeting the requirement of the mean ankle height of about 70 mm [26], the total height of the model is 189 mm. The foot part is Flex-Symes ^{TM}(Össur)

Table 1. Optimized parameters of elastic actuators with the optimized peak mechanical power.

	K_S (Nm/rad)	K_P (Nm/rad)	θ_P (rad)	θ_{UP} (rad)
SEA	971.8411	-	-	-
UPE+SEA	958.1301	242.4056	-	0.1310
PEA	-	318.7666	-0.1649	-
UPEA	-	352.2373	-	-0.1445
SE+PEA	1145.0762	316.6147	-0.1750	-
SE+UPEA	39723.4047	357.2695	-	-0.1428

[27] without a socket adapter.

3. RESULTS

3.1. Optimization of peak mechanical power

With minimizing the peak mechanical power of the motor, the result of PE+SEA, where the stiffness of parallel spring K_P is zero, means PE+SEA cannot provide better optimization than SEA. Parameters of other elastic actuators with effective optimization are shown in Table 1.

Regarding the performance of DDA as the standard (100%), the motor performances of elastic actuators are compared in Fig. 6. On the aspect of optimized power maximum, for basic actuators with a single elastic element, the optimization degree of parallel spring (PEA, 73.06% & UPEA, 74.27%) is considerably better than that of series spring (SEA, 53.66%). Further optimization of the additional elastic element based on the basic actuators is slight. In comparison with the performance of basic actuators, UPE+SEA is 1.38% better than SEA, and the additional series springs in SE+PEA and SE+UPEA improve 1.37% and 0.08% of PEA and UPEA, respectively. On other facets, series spring can reduce the maximum and standard derivation of motor angular velocity, for the best example as UPE+SEA. Parallel springs contribute to the optimization of peak motor torque, and especially the UPE can reduce more than 60% peak torque in UPEA and SE+UPEA. The mean energy consumption powers of all elastic actuators are in the range from 62.12% to 76.39% relative to that of DDA.

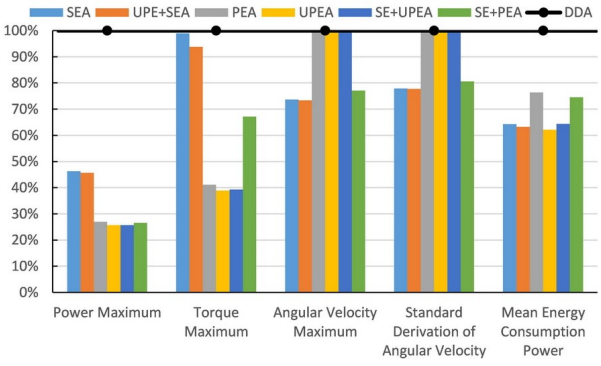

Fig. 6. Motor performances of elastic actuators with the optimized peak mechanical power.

In the case of the peak mechanical power being optimized, the output characteristics of torque, angular velocity, and mechanical power of the transmission in one gait cycle are compared to the data of sound ankle in Fig. 7. There are two different and obvious features on the torque correlated to sound ankle. First, DDA, SEA, and UPE+SEA need more torque. In comparison with DDA, SEA almost cannot provide any optimization of the torque, and UPE+SEA decreases the torque inconsiderably during the gait cycle of 30% to 50%. Second, PEA, SE+PEA, UPEA, and SE+UPEA show an evident offset characteristic towards to positive direction, which stems from the preload generated by the negative equilibrium position of parallel springs. Then, the angular velocity during the stance phase (about 0 to 60% of gait cycle) can be optimized significantly by the low-stiffness series springs in SEA, UPE+SEA, and SE+PEA, although there is an extra fluctuation during 30% to 50% gait; other actuators cannot achieve any optimization of velocity related to DDA. Finally, from the perspective of power, the per-

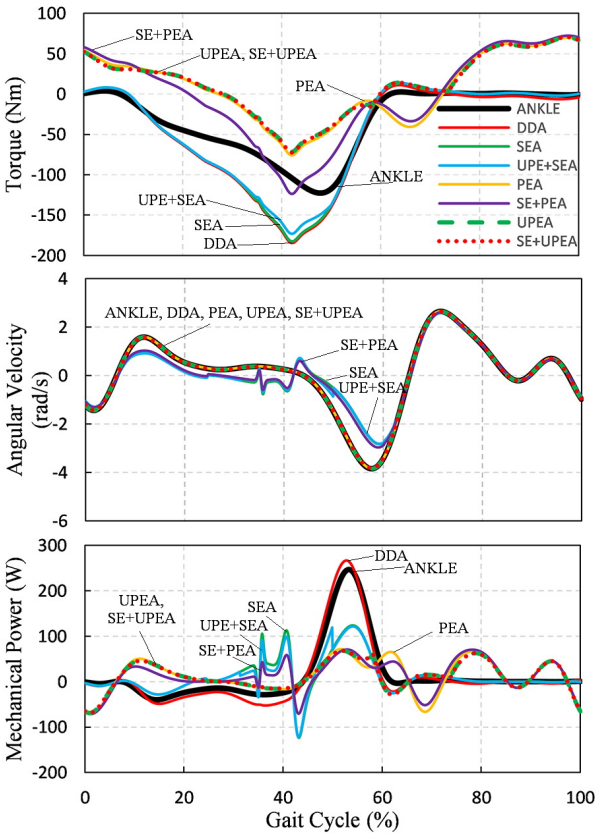

Fig. 7. Output characteristics of transmission with the optimized peak mechanical power.

formance of DDA becomes worse than that of the sound ankle during the whole period. In the 45% and 60% gait, all elastic actuators perform much better than DDA and sound ankle; however, in other phases of gait, there are obvious differences. The powers of SEA and UPE+SEA fluctuate acutely according to the abovementioned fluctuation of velocity; the power fluctuations of PEA, UPEA, and SE+UPEA are evenly distributed in the whole gait; SE+PEA possesses both features of fluctuations.

3.2. Optimization of mean energy consumption power

With minimizing the mean energy consumption power of the motor, the results of UPE+SEA and SE+UPEA, where the stiffness of series spring K_S limits to positive infinity, refer to these two kinds of elastic actuators perform as a UPEA. Parameters of other elastic actuators with effective optimization are shown in Table 2.

Fig. 8 shows the motor performances in diverse particulars of elastic actuators in comparison with DDA (100%). UPEA achieves the most degree of optimization, and the mean energy consumption of UPEA is only 43.27% of DDA; however, its peak mechanical power is more than three-time worse than its optimized peak mechanical power in the first optimization objective as abovementioned. PEA is the worst to optimize the objective, and it can only reduce 31.46% energy consumption. However, almost an extra 10% reduction is obtained by SE+PEA. Meanwhile, the peak mechanical powers of PEA and SE+PEA are 43.49% and 46.73% of DDA.The performances of SEA in two optimization objectives are similar. The optimized mean energy consumption power is only 0.02% better than that under the situation of optimized peak mechanical power, and the difference of power maximum between both optimizations is 1.37%. PE+SEA improves the performance of energy consumption of SEA by about 5.04%. UPEA does the best in reducing the peak torque, and SEA is still preferred in optimizing velocity characteristics with the optimized energy consumption.

Similar to the first optimization objective, when the mean energy consumption of each actuator is optimized, three output characteristics of transmission, that is, torque, angular velocity, and mechanical power, are shown versus the counterparts of the sound ankle in Fig. 9. The comparison of Fig. 7 and Fig. 9 indicates some differences. At the point of torque, the tendency of optimization from PEA and SE+PEA doesn't change a lot, but the degree of optimization changes to a large extent. UPEA reduces the value of torque and even changes the direction of that during the period of UPE operation. On the aspect of velocity, the optimization degree of SE+PEA decreases lightly than that shown in Fig. 7.The addition of parallel spring makes

Table 2. Optimized parameters of elastic actuators with the optimized mean energy consumption power.

	K_S (Nm/rad)	K_P (Nm/rad)	θ_P (rad)	θ_{UP} (rad)
SEA	1001.6424	-	-	-
PE+SEA	1006.6253	25.2982	-	-
PEA	-	202.4897	-0.2143	-
UPEA	-	1033.1387	-	0.0086
SE+PEA	1542.0911	133.0659	-0.1990	-

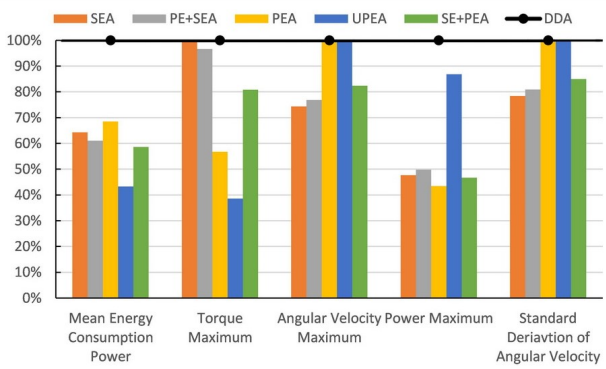

Fig. 8. Motor performances of elastic actuators with the optimized mean energy consumption power.

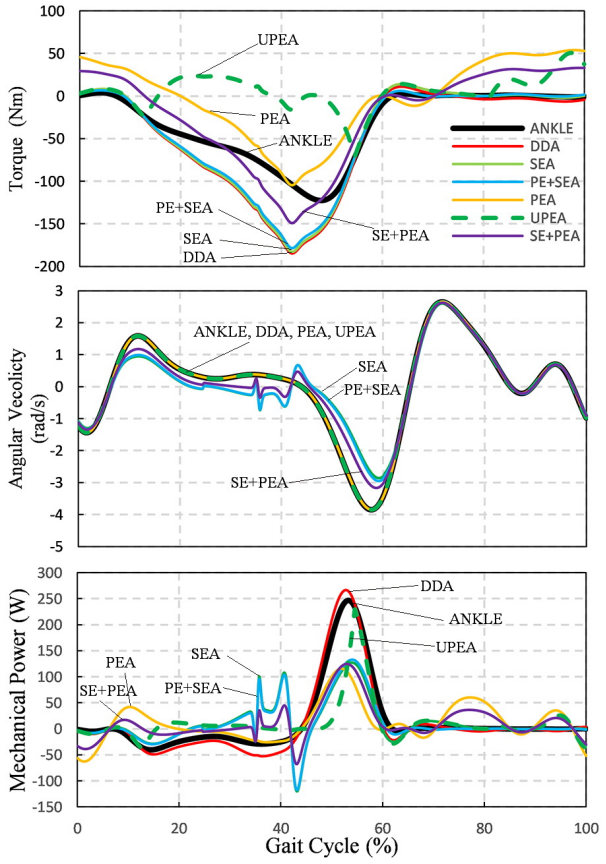

Fig. 9. Output characteristics of transmission with the optimized mean energy consumption power.

PE+SEA have better optimization of energy consumption, although a little part of the optimization of velocity is sacrificed. Finally, UPEA is the only one in which the power tendency is changed considerably to become much similar to the counterparts of DDA and sound ankle. Other elastic actuators keep their features showed with the optimized peak mechanical power.

4. DISCUSSION

The selection and evolution of a 2-DoF vibration system in this study make it possible to analyze and optimize seven kinds of typical elastic actuators at one time. The dynamic models with inertia on the load end also make the analysis closer to the actual operating condition. Therefore, the dynamic models can be applied at different walking or running speeds as long as that the corresponding parameters of the sound ankle are available.

The solution procedure of dynamic models in this work is not based on any specific control system. From the open-loop calculation of optimization, the results of angular velocity and torque that are needed from the output of a motor and transmission only provide a reference to select and confirm the type and specification of components. If an appropriate closed-loop control system is engaged, the actual performance from motor and transmission may be further optimized.

According to the results obtained in the optimization of peak mechanical power, UPEA and its derivative, SE+UPEA, possess the best degree of optimization. Especially, the degree of UPEA is higher than the same actuator called DD+UPS in [12] under similar conditions. The difference may be caused by the preload of UPE being able to exist in this study; hence, the further optimization is achieved. Different from the relationship of UPE+SEA, PE+SEA, and SEA in [12], it is found that the addition of parallel spring in PE+SEA cannot provide obviously better results because the addition of parallel spring will counteract a part of the achievement of velocity optimization from series spring. The optimized results of SEA, PEA, and SE+PEA and the counterparts by the method of the strict-restricted case in [13] are closed to each other, and the inconsiderable difference may come from the impact of different driver mechanism. On the aspect of minimizing the mean energy consumption power, the similarity between the results of UPEA, PEA, and PE+SEA in comparison to SEA and the counterparts in [12] is showed up. However, because there is no specific calculation method of energy consumption in [12], it is impossible to analyze the reason concretely for the differences.

When the results from two different minimizing objectives are compared, it is showed that, except two results of SEA are analogous, the unconformity happens in PEA, UPEA, and SE+PEA. An example of UPEA is that, when peak mechanical power is minimized, the peak mechanical power and the mean energy consumption power are 107.18 W and 40.54 W, respectively. However, when the mean energy consumption power is optimized to 28.24 W, the peak mechanical power gets much worse to 361.74 W. Therefore, it is necessary to make a trade-off between the two features, namely between the size of the motor and the capacity of the battery in the prosthesis.

Other performances can also be regarded as the selection criteria of elastic actuators. About the optimization of peak torque, the UPEA or SE+UPEA provides a favorable solution when the utilization of a prosthesis requires greater torque output, e.g., the off-board experiment prosthesis [28,29] or the prosthesis for the users with a great weight. The standard deviation of motor speed reflects the acuteness of the variation of angular velocity. In general, the variation of motor speed may cause mechanical vibrations in the prosthesis that makes its wearers uncomfortable. Therefore, in this case, SEA or UPE+SEA that possess the lowest standard deviation can be applied in some transitional products for new users of a prosthesis.

5. CONCLUSION

This study constructs the dynamic models of seven kinds of typical elastic actuators applied in powered ankle-foot prostheses based on a 2-DoF vibration system. Two objectives that are to minimize the peak mechanical power and mean energy consumption power of motor are optimized, respectively, with the selected parameters of physiology and walking. Optimized characteristics of motor power and corresponding characteristics of torque and angular velocity of motors in elastic actuators are compared to the counterparts of DDA, while output characteristics of transmission are also contrasted with the data of sound ankle. The results of this study contribute to understand the optimization mechanism of different elastic elements in the corresponding elastic actuators and provide a valid reference to the selection of an elastic actuator during the design of a powered ankle-foot prosthesis.

The future work will include but not limit to several aspects. First, different elastic actuators will be applied to the new design of powered ankle-foot prostheses for different target users, according to their advantages. During the process of design, the results of this study will be further verified by bench-top and clinical experiments. Second, the dynamic models of elastic actuators will be improved further to involve more elements, such as damping of elastic elements and frictional force inside the whole system, so that the analysis will be closer to the actual situation in some cases that need high accuracy. Third, different and more complicate working conditions of the ankle-foot prosthesis, such as running or crouch walking, will be considered to explore whether elastic actuators will perform differently. Finally, if possible, applications of elas-

tic actuators compared in this study will be explored in more fields, such as transfemoral prosthesis, exoskeleton orthotics, or other medical robots.

REFERENCES

[1] G. A. Pratt and M. M. Williamson, "Series elastic actuators," *Proc. of IEEE/RSJ International Conference on Intelligent Robots and Systems, Human Robot Interaction and Cooperative Robots*, pp. 399-406, 1995.

[2] E. Shata, K.-D. Nguyen, P. Acharya, and J. Doom, "A series-elastic robot for back-pain rehabilitation," *International Journal of Control, Automation and Systems*, vol. 19, no. 2, pp. 1054-1064, February 2021.

[3] J. Liu, N. A. Abu Osman, M. Al Kouzbary, H. Al Kouzbary, N. A. Abd Razak, H. N. Shasmin, and N. Arifin, "Classification and comparison of mechanical design of powered ankle-foot prostheses for transtibial amputees developed in the 21st century: A systematic review," *Journal of Medical Devices*, vol. 15, no. 1, p. 010801, March 2021.

[4] M. Grimmer, M. Holgate, R. Holgate, A. Boehler, J. Ward, K. Hollander, T. Sugar, and A. Seyfarth, "A powered prosthetic ankle joint for walking and running," *Biomedical Engineering Online*, vol. 15, p. 141, December 2016.

[5] S. K. Au and H. M. Herr, "Powered ankle-foot prosthesis," *IEEE Robotics Automation Magazine*, vol. 15, no. 3, pp. 52-59, September 2008.

[6] A. Fu, C. Fu, K. Wang, D. Zhao, X. Chen, and K. Chen, "The key parameter selection in design of an active electrical transfemoral prosthesis," *Proc. of IEEE International Conference on Robotics and Biomimetics (ROBIO)*, pp. 1716-1721, 2013.

[7] J. K. Hitt, T. G. Sugar, M. Holgate, and R. Bellman, "An active foot-ankle prosthesis with biomechanical energy regeneration," *Journal of Medical Devices*, vol. 4, no. 1, p. 011003, March 2010.

[8] E. J. Rouse, N. C. Villagaray-Carski, R. W. Emerson, and H. M. Herr, "Design and testing of a bionic dancing prosthesis," *PloS one*, vol. 10, no. 8, p. e0135148, August 2015.

[9] H. Sha, J. Li, W. Li, H. Zhang, H. Hu, C. Li, and H. Guo, "Dynamic analysis and optimization for the ankle joint prosthesis," *Proc. of IEEE International Conference on Rehabilitation Robotics (ICORR)*, pp. 283-288, 2015.

[10] C. Lee, S. Kwak, J. Kwak, and S. Oh, "Generalization of series elastic actuator configurations and dynamic behavior comparison," *Actuators*, vol. 6, no. 3, p. 26, August 2017.

[11] T. Verstraten, P. Beckerle, R. Furnmont, G. Mathijssen, B. Vanderborght, and D. Lefeber, "Series and parallel elastic actuation: Impact of natural dynamics on power and energy consumption," *Mechanism and Machine Theory*, vol. 102, no., pp. 232-246, May 2016.

[12] M. Eslamy, M. Grimmer, and A. Seyfarth, "Effects of unidirectional parallel springs on required peak power and energy in powered prosthetic ankles: Comparison between different active actuation concepts," *Proc. of IEEE International Conference on Robotics and Biomimetics (ROBIO)*, pp. 2406-2412, 2012.

[13] M. Grimmer, M. Eslamy, S. Gliech, and A. Seyfarth, "A comparison of parallel-and series elastic elements in an actuator for mimicking human ankle joint in walking and running," *Proc. of IEEE International Conference on Robotics and Automation*, pp. 2463-2470, 2012.

[14] E. a. B. Nieto, S. Rezazadeh, and R. D. Gregg, "Minimizing energy consumption and peak power of series elastic actuators: A convex optimization framework for elastic element design," *IEEE/ASME Transactions on Mechatronics*, vol. 24, no. 3, pp. 1334-1345, March 2019.

[15] E. Bolívar, S. Rezazadeh, and R. Gregg, "A general framework for minimizing energy consumption of series elastic actuators with regeneration," *Proc. of Dynamic Systems and Control Conference*, p. V001T036A005, 2017.

[16] P. Zhao, "Dynamitic model and characteristics analysis of series elastic actuator," M. Eng, Harbin Engineering University, Harbin, China, 2012.

[17] M. Al Kouzbary, N. A. Abu Osman, H. Al Kouzbary, H. N. Shasmin, and N. Arifin, "Towards universal control system for powered ankle-foot prosthesis: A simulation study," *International Journal of Fuzzy Systems*, vol. 22, no. 4, pp. 1299-1313, April 2020.

[18] D. A. Winter, *Biomechanics and Motor Control of Human Gait: Normal, Elderly and Pathological*, University of Waterloo Press, Waterloo, Canada, 1991.

[19] E. J. Rouse, L. J. Hargrove, E. J. Perreault, and T. A. Kuiken, "Estimation of human ankle impedance during the stance phase of walking," *IEEE Transactions on Neural Systems Rehabilitation Engineering*, vol. 22, no. 4, pp. 870-878, February 2014.

[20] H. Lee and N. Hogan, "Time-varying ankle mechanical impedance during human locomotion," *IEEE Transactions on Neural Systems Rehabilitation Engineering*, vol. 23, no. 5, pp. 755-764, August 2014.

[21] A. L. Shorter and E. J. Rouse, "Mechanical impedance of the ankle during the terminal stance phase of walking," *IEEE Transactions on Neural Systems Rehabilitation Engineering*, vol. 26, no. 1, pp. 135-143, September 2017.

[22] G. D. Tao, *Mechanical Bracing Solutions to Decrease Tibial Slippage of Anklebot*, B.S. Thesis, Massachusetts Institute of Technology, Cambridge, Massachusetts, 2010.

[23] M. L. Palmer, *Sagittal Plane Characterization of Normal Human Ankle Function Across a Range of Walking Gait Speeds*, M.S. Thesis, Massachusetts Institute of Technology, Cambridge, Massachusetts, 2002.

[24] M. H. Ahmed, F. Wahid, A. Ali, M. I. Tiwana, J. Iqbal, and N. H. Lovell, "Actuator design for robotic powered an ankle-foot prosthesis," *Proc. of International Symposium on Bioelectronics and Bioinformatics (ISBB)*, pp. 136-139, 2015.

[25] M. F. Eilenberg, H. Geyer, and H. Herr, "Control of a powered ankle-foot prosthesis based on a neuromuscular model," *IEEE Transactions on Neural Systems Rehabilitation Engineering*, vol. 18, no. 2, pp. 164-173, January 2010.

[26] C. Wang, D. Wang, X. Bai, J. Wang, and G. Tang, *Biomechanics of the Human Bone-muscle System*, Chinese Science Publishing, Beijing, China, 2015.

[27] "Flex-symes™(Össur)," https://www.ossur.com/en-gb/prosthetics/feet/flex-symes

[28] J. M. Caputo and S. H. Collins, "A universal ankle-foot prosthesis emulator for human locomotion experiments," *Journal of Biomechanical Engineering*, vol. 136, no. 3, p. 035002, March 2014.

[29] S. H. Collins, M. Kim, T. Chen, and T. Chen, "An ankle-foot prosthesis emulator with control of plantarflexion and inversion-eversion torque," *Proc. of IEEE International Conference on Robotics and Automation (ICRA)*, pp. 1210-1216, 2015.

Jingjing Liu received his B.S. degree in mechanical design manufacture and its automation from Tongji University in 2010, followed by an M.S. degree in biomedical engineering from University of Shanghai for Science and Technology. He is currently pursuing a doctoral degree from University of Malaya. His research interets include the design and development of powered ankle-foot prosthesis, and the biomechanics analysis from prosthesis to human body.

Noor Azuan Abu Osman graduated from University of Bradford, United Kingdom with his B.Eng. Hons. in mechanical engineering, followed by his M.Sc. and Ph.D. degrees in bioengineering from University of Strathclyde, United Kingdom. Practicing Engineer and Professor of Biomechanics with Faculty of Engineering, University of Malaya, Malaysia. His research interests are quite wide-ranging under the general umbrella of biomechanics. However, his main interests are the measurements of human movement, prosthetics design, the development of instrumentation for forces and joint motion, and the design of prosthetics, orthotics and orthopaedic. Prior to joining University of Malaya, Malaysia in 1996, he worked as Mechanical and Electrical Engineer and actively involved in many consultancy projects, especially in the field of biomechanics and bio-mechanical engineering.

Mouaz Al Kouzbary received his B.Sc. degree in mechatronics engineering from the University of Aleppo, Syria, and his M.Eng.Sc. degree in biomedical engineering from the University of Malaya, Malaysia. He is currently a Ph.D. candidate and research assistance at the Centre for Applied Biomechanics (CAB), Department of Biomedical Engineering, Faculty of Engineering, University of Malaya. His research interests include Artificial Intelligent control systems, machine learning algorithms, genetic algorithm, robotics, biomechanics, powered lower limb prostheses, and bio-inspired leg designs.

Hamza AL Kouzbary received his B.Sc. degree in mechatronics engineering from the University of Aleppo, Syria in 2017. In 2018 he joined the department of biomedical engineering at the University of Malaya as a Master of Engineering Science (research program) student and research assistance. His research interests include rehabilitation robots, bipedal robots, Artificial intelligent and control systems.

Nasrul Anur Abd Razak received his B.Eng. degree in mechatronics from International Islamic University Malaysia, Selangor, Malaysia in 2009 followed by his M.Eng. and Ph.D. degrees from Department of Biomedical Engineering, University Malaya, Kuala Lumpur, Malaysia in (2011) and (2014). Since (2015), he has been a Senior Lecturer at Department of Department of Biomedical Engineering, Faculty of Engineering, University Malaya, Kuala Lumpur, Malaysia. His research interests include biomechanical engineering (manufacturing in prosthetics, bio sculptor CAD/CAM system), prosthetics and orthotics engineering, and rehabilitation engineering (upper limb prosthetic, assistive devices & technology in prosthetic and orthotics, biomechatronic in prosthetic and orthotics).

Hanie Nadia Shasmin received her B.Eng. degree in biomedical engineering from the University of Malaya, Kuala Lumpur, Malaysia, in 2006. She has been a Research Officer with the University of Malaya, since 2012, where she is currently affiliated with the Centre for Applied Biomechanics, Faculty of Engineering. Her research interests include biomechanics, motion analysis, gait and rehabilitation.

Nooranida Arifin is a senior lecturer at the University of Malaya. She received her B.Sc. and Ph.D. degrees in biomedical engineering from the University of Malaya and her M.Sc. degree in prosthetics and orthotics from Eastern Michigan University, Michigan, USA. Her current research interests cover prosthetics and orthotics biomechanics, in particular, focusing on the balance mechanism with prosthetics intervention following lower-limb amputation. She is an active member of the International Society for Prosthetics Orthotics, Malaysia.